Islamic Azad University

Journal of

Optoelectronical Nanostructures

Winter 2018 / Vol. 3, No. 1

Investigation of the Third-Order Nonlinear Optical Susceptibilities and Nonlinear Refractive Index In Pbs/Cdse/Cds Spherical Quantum Dot

Fatemeh Rahmani[1], Javad Hasanzadeh[*,1]

[1]Department of Physics, Takestan Branch, Islamic Azad University, Takestan, Iran

(Received 24 Dec. 2017; Revised 28 Jan. 2018; Accepted 21 Feb. 2018; Published 15 Mar. 2018)

Abstract: In this study the third order nonlinear susceptibilities are theoretically calculated for an electron confined in an isolated PbS/ CdSe/ CdS spherical core-shell-shell quantum dots. Our calculation is associated with intersubband transitions in the conduction band. We used the effective mass approximation in this study which is a simple and straightforward study of the third-order optical nonlinearity in nanometersized parabolic quantum dots and solved a three-dimensional Schrödinger equation. The third order nonlinear susceptibilities are analyzed as function of core, shell radii. Our study show great dependence of third order nonlinear susceptibilities on size of core and shell. Also In the case of Kerr-type nonlinearities, nonlinear refractive index n_2 and the nonlinear absorption coefficient β are investigated as function of the ratio k_0/n_0 (where n_0 and k_0 are the real and imaginary part of linear refractive index respectively) for different value of imaginary and real parts of the third order susceptibility.

Key words: Core–Shell-Shell Quantum Dot, Nonlinear Optical Susceptibility, Nonlinear Refractive Index.

1. INTRODUCTION

In the recent years, many researchers have studied on synthesis of spherical quantum dot with a core in center and one or several layers of called core–shell structure QD or quantum dot–quantum well (QDQW) [1]. In recent years, third-order nonlinear optical susceptibilities associated with intersubband transitions in the conduction band in various types of semiconductor nanoparticles have been investigated [2-4].

* Corresponding author. E-mail: **j.hasanzadeh@tiau.ac.ir**

Semiconductors have promising applications in optoelectronic and photonic devices. Among them, PbS is one of the important IV–VI group semiconductors having a narrow band gap (E_g = 0.41 eV) with an effective Bohr radius of 18 nm. The band gap can be tuned for absorption across the visible to near infrared (NIR) regions (700–1600 nm). Materials exhibiting NIR absorption and emission are very useful in various applications like NIR communications, in vivo biomedical applications (imaging and labelling), infrared detectors and electroluminescent devices [5].
Some researchers investigated core/shell or cylinder quantum dots [6-8] but we have calculated the third-order susceptibility in PbS/CdSe/CdS core/shell/shell quantum dot also we have investigated the refractive index and the absorption coefficient using Kerr-type nonlinearities which has not been studied so far.

2. THOERY AND CANCLUSION

In this paper, we have considered the system of an electron confined in an isolated PbS/CdSe/CdS core/shell/shell quantum dot inner radius R_1 and two outer radii R_2 and R_3 corresponding to the PbS (as core), CdSe (as first shell) and CdS (as second shell) respectively as shown in Fig. 1.

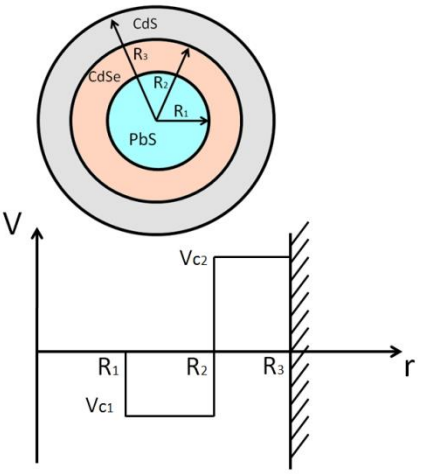

Fig.1. Two-dimensional model and the potential diagram of the PbS/CdSe/CdS spherical quantum dot.

Various methods have been reported for investigating electronic structures of quantum dot systems. We used the effective mass approximation in this study. The time independent Schrödinger equation of the electron in spherical coordinate can be written as [9].

$$(-\frac{\hbar^2}{2m_i^*}\nabla^2 - V_i)\psi_{nlm} = E\psi_{nlm}$$

$$\left[-\frac{\hbar^2}{2m_{i.e.(h)}r^2}\left[\frac{\partial}{\partial r}\left(r^2\frac{\partial}{\partial r}\right) + \frac{1}{sin\,\theta}\frac{\partial}{\partial\theta}\left(sin\,\theta\frac{\partial}{\partial\theta}\right) + \frac{1}{sin^2\,\theta}\frac{\partial^2}{\partial\varphi^2}\right] + V_i\right]\psi_{nlm}(r,\theta,\varphi) =$$

$$E\psi_{nlm}(r,\theta,\varphi) \quad (1)$$

Where m_i^* is the effective mass of an electron in the i_{th} th region, and $V_i(r)$ is the potential. They are obtained as follows:

$$m_i^* = \begin{cases} m_1^* & r \le R_1 \\ m_2^* & R_1 < r \le R_2 \\ m_3^* & R_2 < r \le R_3 \end{cases} \quad (2)$$

$$V_c(r) = \begin{cases} 0 & 0 < r \le R_1 \\ V_{c1} & R_1 < r \le R_2 \\ V_{c2} & R_2 < r \le R_3 \\ \infty & r > R_3 \end{cases} \quad (3)$$

Where $V_{c1} = \chi_1 - \chi_2$ and $V_{c2} = \chi_2 - \chi_3$. χ_1, χ_2 and χ_3 are electron affinity of PbS, CdSe and CdS respectively. Fig. 2 shows the schematic representation of the band structure of PbS/CdSe/CdS core–shell-shell quantum dots. The value of electron affinity, effective mass and band gap of materials are given in table 1.

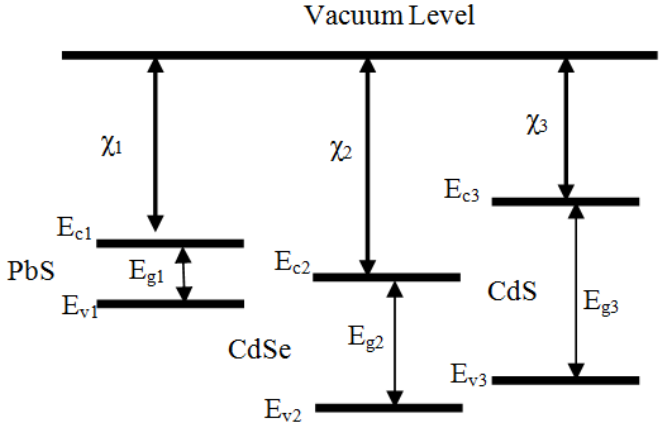

Fig. 2. Schematic energy band representation of PbS/CdSe/CdS spherical quantum dot.

Table1. Electron affinity, effective mass and band gap of PbS, CdSe and CdS [10-14]

	Electron Affinity(eV)	Effective mass of electron	Band gap(eV)
PbS	4.6[7,9]	$0.25m_0$ [8]	0.41
CdSe[10]	4.95	$0.13m_0$	1.75
CdS[11]	4.3	$0.171m_0$	2.42

The separation of radial and angular coordinates leads to:

$$\psi_{nlm}(r,\theta,\varphi) = R_{nl}(r)Y_{l,m}(\theta,\varphi) \quad (4)$$

R_{nl}(r) is the radial wave function, and $Y_{lm}(\theta, \phi)$ is the spherical harmonic function and is the solution of the angular part of the Schrödinger equation, and l and m are the angular momentum quantum numbers.

According to Fig.1, there are four regions for electron eigenenergy; $E < V_{c1}$, $V_{c1} < E < V_{c2}$, $E > V_{c2}$. In this paper we consider $V_{c1} < E < V_{c2}$ & $E > 0$. For this case the solution of R_{nl}(r) yields [15]:

$$R_{n,l}(r) = \begin{cases} A_1 j_l(k_{nl,1}r) + A_2 n_l(k_{nl,1}r) & r \le R_1 \\ B_1 j_l(k_{nl,2}r) + B_2 n_l(k_{nl,2}r) & R_1 < r \le R_2 \\ C_1 h_l^{(+)}(ik_{nl,3}r) + C_2 h_l^{(-)}(ik_{nl,3}r) & R_2 < r \le R_3 \\ 0 & r > R_3 \end{cases} \quad (5)$$

Where A_1, A_2, B_1, B_2, C_1 and C_2 are normalized constants, and $k_{nl,1}$, $k_{nl,2}$, $k_{nl,3}$ apply to the following equations:

$$k_{nl,1} = \sqrt{\frac{2m_1^* E}{\hbar^2}}$$
$$k_{nl,2} = \sqrt{\frac{2m_2^*(E-V_{c1})}{\hbar^2}} \quad (6)$$
$$k_{nl,3} = \sqrt{\frac{2m_3^*(E-V_{c2})}{\hbar^2}}$$

Due to the fact that the wave function is finite for $r \to 0$, we can get $A_2 = 0$. Also, the wave function must satisfy the boundary conditions [16, 17]:

$$R_{nl,1}(R_1) = R_{nl,2}(R_1)$$
$$R_{nl,2}(R_2) = R_{nl,3}(R_2)$$
$$\frac{1}{m_1^*}\frac{dR_{nl,1}(r)}{dr}\Big|_{r=R_1} = \frac{1}{m_2^*}\frac{dR_{nl,2}(r)}{dr}\Big|_{r=R_2} \quad (7)$$
$$\frac{1}{m_2^*}\frac{dR_{nl,2}(r)}{dr}\Big|_{r=R_2} = \frac{1}{m_3^*}\frac{dR_{nl,3}(r)}{dr}\Big|_{r=R_3}$$
$$\int_0^{R_1} r^2 R_{nl,1}^* R_{nl,1}\, dr + \int_{R_1}^{R_2} r^2 R_{nl,2}^* R_{nl,2}\, dr + \int_{R_2}^{R_3} r^2 R_{nl,3}^* R_{nl,3}\, dr = 1$$

After determining the eigenvalues and wave functions, the third-order susceptibility for two energy levels, ground and first excited states, we shal describe the model By using the density matrix method [18], the third order

optical nonlinearity susceptibility $\chi^{(3)}$ corresponding to four wave mixing in a two-level model reads [19]:

$$\chi^{(3)}(-2\omega_1+\omega_2;\omega_1,\omega_1,-\omega_2)=\frac{-2i\mu^4N}{[i\hbar(\omega_0-2\omega_1+\omega_2)+\hbar\gamma(i\hbar(\omega_2-\omega_1)+\hbar\gamma_{\|})]}\times\left[\frac{1}{[i\hbar(\omega_0-\omega_1)\hbar\gamma_{\perp}]}+\frac{1}{[i\hbar(\omega_2-\omega_0)+\hbar\gamma_{\perp}]}\right] \quad (8)$$

Where μ is the dipole transition matrix element, ω_0 the transition frequency, $\gamma_{\perp}$($\gamma_{||}$) the transverse (longitudinal) relaxation constant, and N the electron density. In this paper, we suppose $\gamma_{\perp} = \gamma_{\|} = \gamma = 1/\tau$, τ is the relaxation time. The transition frequency $\omega 0$ and dipole transition matrix element μ can be written as:

$$\mu = < \phi_i|er|\phi_j > \quad , \quad \omega_0 = \frac{E_j - E_i}{\hbar} \quad (9)$$

If $\omega_1 = -\omega_2$, the third-order susceptibility for third harmonic generation will be emerge [20].

3. RESULTS AND DISCUSSION

In this paper, only the situation ω_1=0 and ω_2= -ω for the quadratic electro – optic effects (QEOE) have been considered. The material parameters in our calculation have been taken from table 1 and we opt to consider N=$5 \times 10^{24} m^{-3}$, $\tau =$ 300fs [7].

In Fig. 3, we display $\left|\chi^{(3)}(-\omega;0,0,\omega)\right|$, $Re\chi^{(3)}(-\omega;0,0,\omega)$ and $Im\chi^{(3)}(-\omega;0,0,\omega)$ as a function of pump photon energy $\hbar\omega$ for different inner radius (R_1) with a fixed outer radii (R_2 , R_3). $Re\chi^{(3)}(-\omega;0,0,\omega)$ and $Im\chi^{(3)}(-\omega;0,0,\omega)$ responsible for the direct current (DC) Kerr effect and the electro-absorption process, respectively [7]. As shown in Fig. 3, there is one peak which is due to single photon resonance. Also, the susceptibility value and the peak value take a red shift effectively when R_1 increases. This is a consequence of the quantum size effect. When R increases, energy distances between electronic states (i.e., ω_0 in Eq. (14)) in the conduction band become smaller. In the following, dipole matrix element μ becomes stronger with the increase of the radius [8]. As shown in Figs. 3(b) and 3(c), near the resonant frequency, $Re\chi^{(3)}(-\omega;0,0,\omega)$ changes its sign from $-4\times10^{-12}\, m^2/V^2$ to Similar to $+4\times10^{-12}\, m^2/V^2$ but $Im\chi^{(3)}(-\omega;0,0,\omega)$ always keeps negative. Also we see, $Im\chi^{(3)}(-\omega;0,0,\omega)$ fast reaches negative maximum $-8\times10^{-12}\, m^2/V^2$ when frequency slightly increases. This is similar to reports by

[7, 21]. These are important for the further development of quantum dots optical nonlinear devices [18].

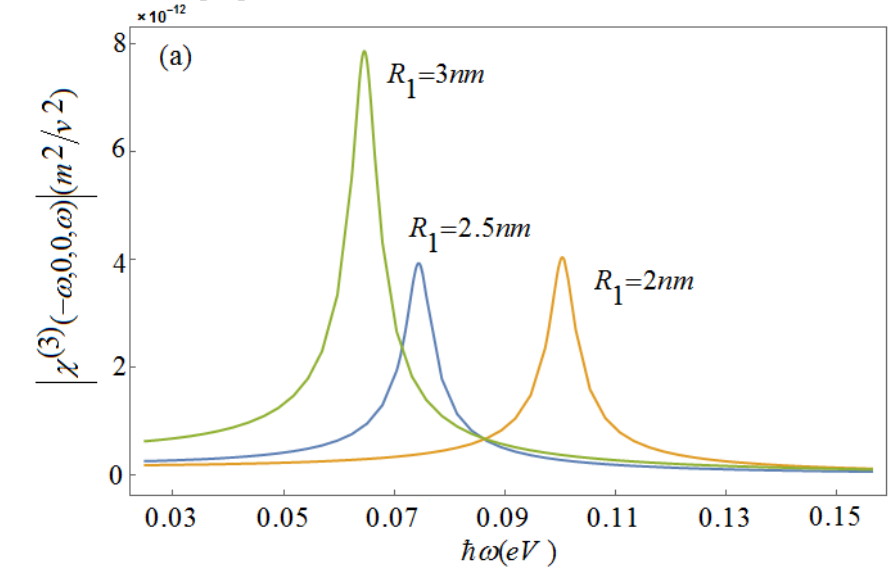

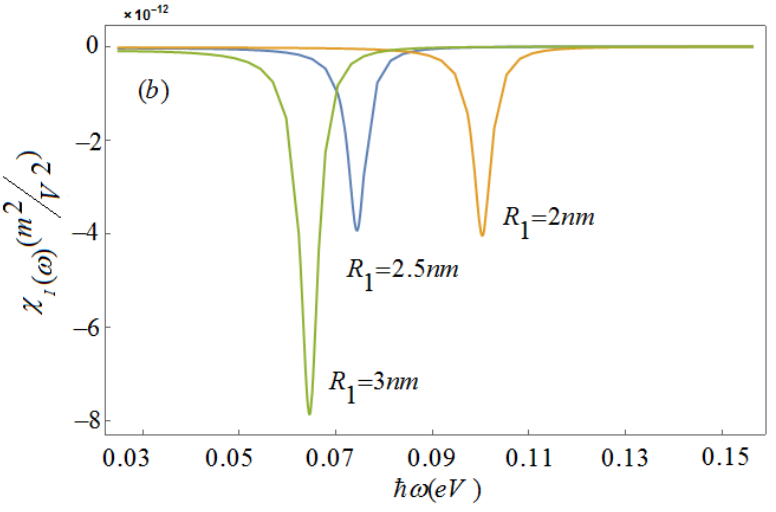

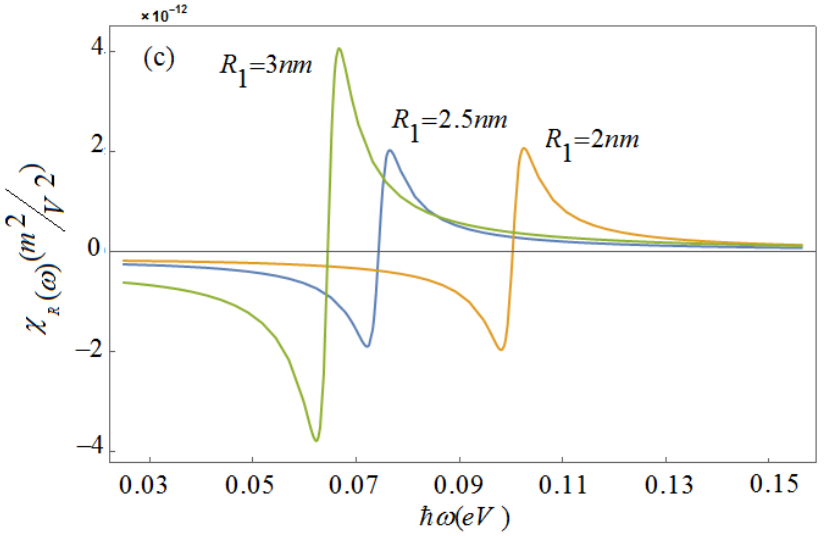

Fig.3. The modulus (a), imaginary part (b) and real part (c) of $\chi^{(3)}(-\omega;0,0,\omega)$ versus the pump photon energy with different R_1 and fixed R_2 and R_3 (R2=4nm, R3=5nm).

Figs. 4 and 5 show $\left|\chi^{(3)}(-\omega;0,0,\omega)\right|$, $Re\chi^{(3)}(-\omega;0,0,\omega)$ and $Im\chi^{(3)}(-\omega;0,0,\omega)$ as a function of pump photon energy $\hbar\omega$ for different R_2 (with a fixed R_1, R_3) and different R_3 (with a fixed R_1 , R_2) respectively.
Comparing Fig. 5 with Fig. 4, we found that the susceptibilities increase more slowly and the peak shift much less for different values of R_2 than for different values of R_1. We showed that the susceptibilities increase much slowly and the peak shift much less for different values of R_3.

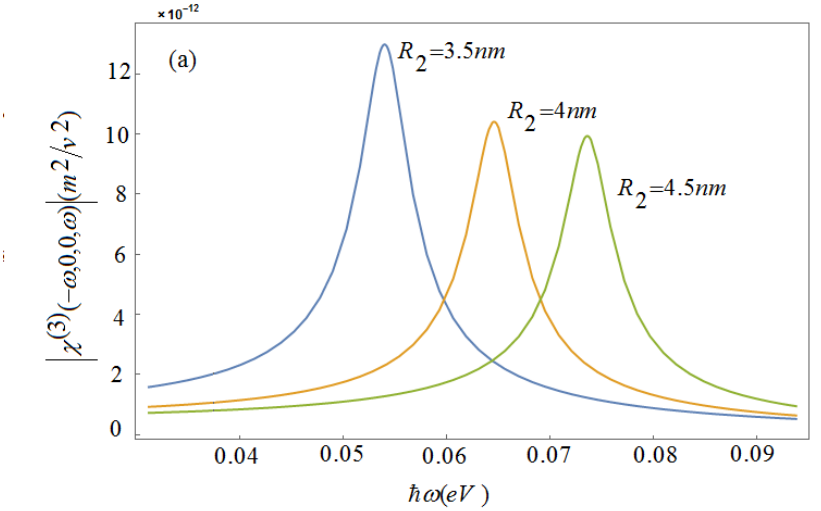
×10⁻¹²
(a)
R_2=3.5nm
R_2=4nm
R_2=4.5nm
$\left|\chi^{(3)}(-\omega,0,0,\omega)\right|(m^2/v^2)$
0
2
4
6
8
10
12
0.04
0.05
0.06
0.07
0.08
0.09
$\hbar\omega(eV)$

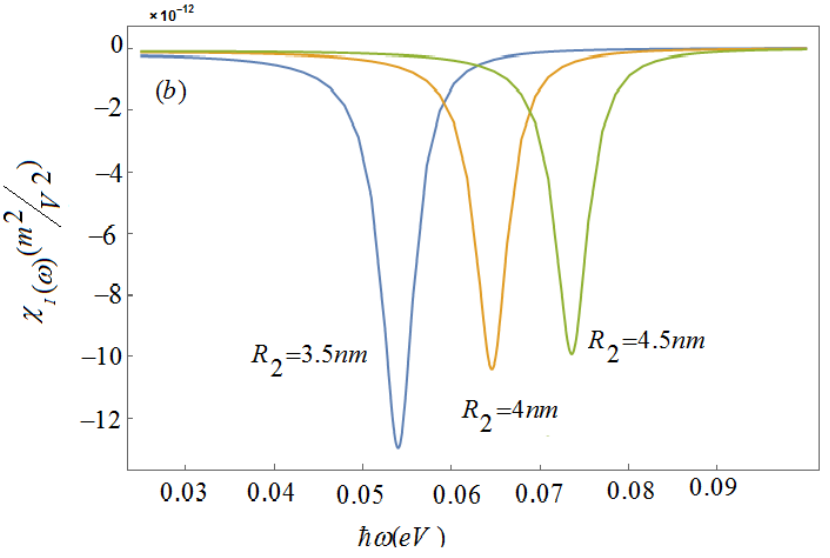
×10⁻¹²
(b)
$\chi_I(\omega)(m^2/v^2)$
0
−2
−4
−6
−8
−10
−12
R_2=3.5nm
R_2=4nm
R_2=4.5nm
0.03
0.04
0.05
0.06
0.07
0.08
0.09
$\hbar\omega(eV)$

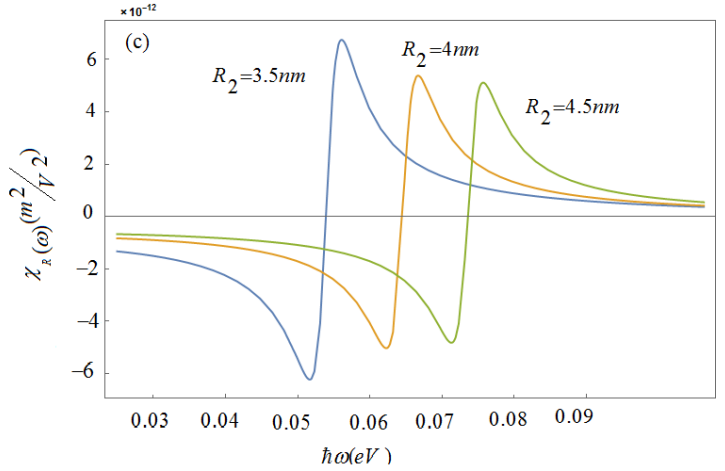

Fig.4. The modulus (a), imaginary part (b) and real part (c) of $\chi^{(3)}(-\omega;0,0,\omega)$ versus the pump photon energy with different R_2 and fixed R_1 and R_3 (R1=3nm, R3=5nm).

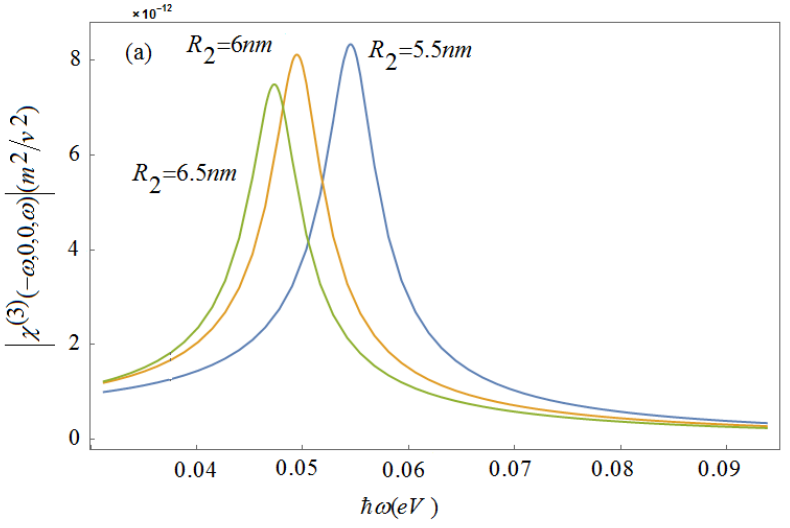

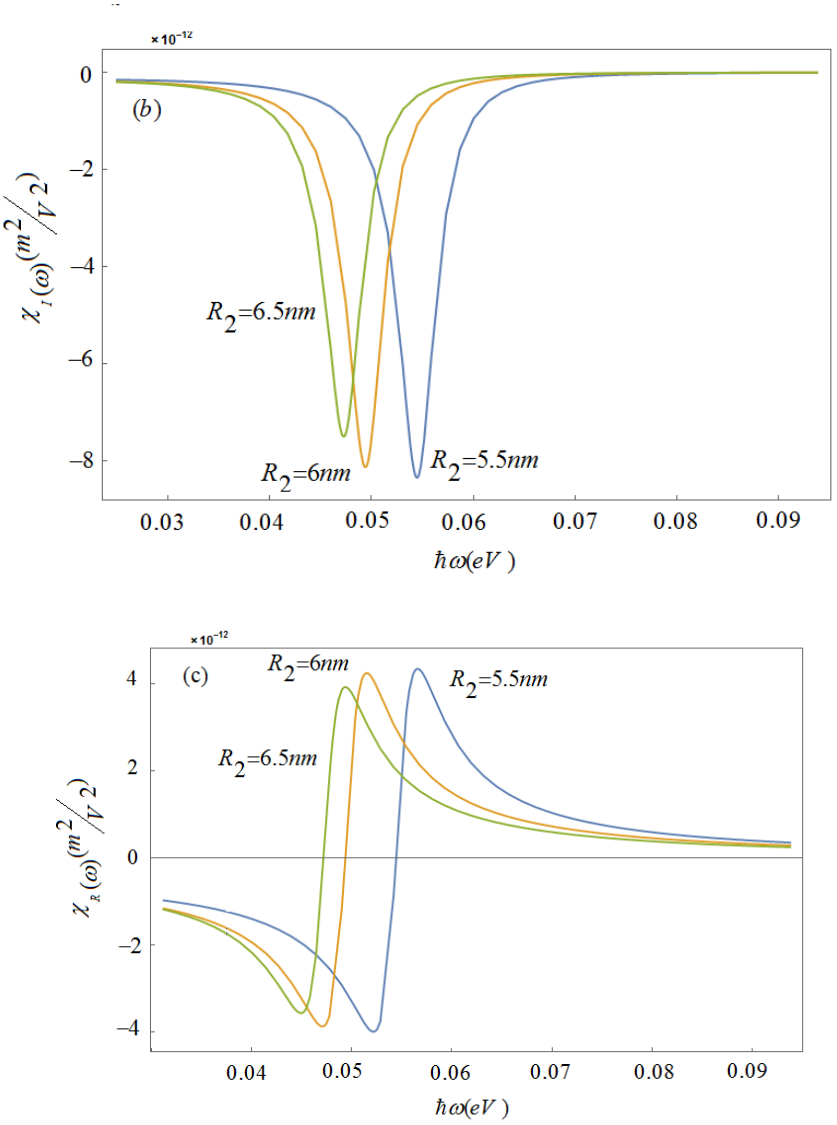

Fig.5. The modulus (a), imaginary part (b) and real part (c) of $\chi^{(3)}(-\omega;0,0,\omega)$ versus the pump photon energy with different R_3 and fixed R_1 and R_2 (R1=3nm, R2=4nm).

The interesting thing in Figs 4 is that by increasing the size of the shell 1, blue shift can be seen in the diagram. This can be due to the negative value for V_C in the shell 1 which means it functions as a quantum well.

Comparing Figures 4 and 5, we can see that the shift of the peak in Figure 4, with the increase in R_2 (R_1 and R_3 : fixed) is less than the shift of the peak in Figure 5, where R_3 (R_1 and R_2 : fixed) is intentionally increased. This may be due to the fact that in case of $E>V_c$ electrons can penetrate from shell barrier region to the shell layer. Because compared to shell 2, shell 1 acts as a well. Consequently, electrons are more confined in the well.

In the case of Kerr-type nonlinearities, the expressions relating to the refractive index and the absorption coefficient with the intensity I of the electromagnetic wave are $n = n_0 + n_2 I$ and $\alpha = \alpha_0 + \beta I$, where n_0 and α_0 are the linear refractive index and linear absorption coefficient, respectively. In a system showing a negligible absorption ($\alpha_0 = 0$), the nonlinear refractive index n_2 and the nonlinear absorption coefficient β are proportional to the real $\chi_R^{(3)}$ and imaginary $\chi_I^{(3)}$ parts of $\chi^{(3)}$ through the following expressions [22]:

$$n_2 = \frac{3}{4\varepsilon_0 c(n_0^2 + k_0^2)}\left[x_R^{(3)} + \frac{k_0}{n_0}x_I^{(3)}\right]$$
$$\beta = \frac{3\pi}{\lambda\varepsilon_0 c(n_0^2 + k_0^2)}\left[x_I^{(3)} - \frac{k_0}{n_0}x_R^{(3)}\right] \quad (10)$$

Where ε_0 , λ are electric permittivity of free space and the wavelength respectively and $k_0 = \lambda\alpha_0/4\pi$ is related to $k = k_0 + k_2$ I where k denotes the imaginary part of the refractive index. The ratio of n_2 and $n_2(k_0 = 0)$ can be obtained as follows:

$$\frac{n_2}{n_2(k_0=0)} = \left(1 + \frac{k_0^2}{n_0^2}\right)^{-1}\left[1 + \frac{k_0}{n_0}\frac{x_I^{(3)}}{x_R^{(3)}}\right] \quad (11)$$

By the same token,

$$\frac{\beta}{\beta(k_0=0)} = \left[1 + \frac{k_0^2}{n_0^2}\right]^{-1}\left[1 - \frac{k_0}{n_0}\frac{x_R^{(3)}}{x_I^{(3)}}\right] \quad (12)$$

Remarkably, this ratio is dependent on the ratios of the absorption coefficient and the refractive index k_0/n_0 and the imaginary and real parts of the third order susceptibility $\chi_I^{(3)}/\chi_R^{(3)}$.

Fig. 6 shows the ratio $n_2/n_{2(k0=0)}$ and $\beta/\beta_{(k0=0)}$ have been plotted as a function of the ratio k_0/n_0 for different values (positive and negative) of the ratio $\chi_I^{(3)}/\chi_R^{(3)}$ in sample (R_1 = 3nm, R_2 = 4nm and R_3 = 5nm) respectively. As we seen, the variation of ratio $n_2/n_{2(k0=0)}$ and $\beta/\beta_{(k0=0)}$ versuss k_0/n_0 are the same for all $\chi_I^{(3)}/\chi_R^{(3)}$ up to k_0/n_0 =1, while $n_2/n_{2(k0=0)}$ ($\beta/\beta_{(k0=0)}$) drops drastically by decreasing (increasing) of $\chi_I^{(3)}/\chi_R^{(3)}$ after k_0/n_0 =1 so that ratio $n_2/n_{2(k0=0)}$ and $\beta/\beta_{(k0=0)}$ fall down nearly vertically for $\chi_I^{(3)}/\chi_R^{(3)}$ = -0.392 and $\chi_I^{(3)}/\chi_R^{(3)}$ =0.645 respectively.

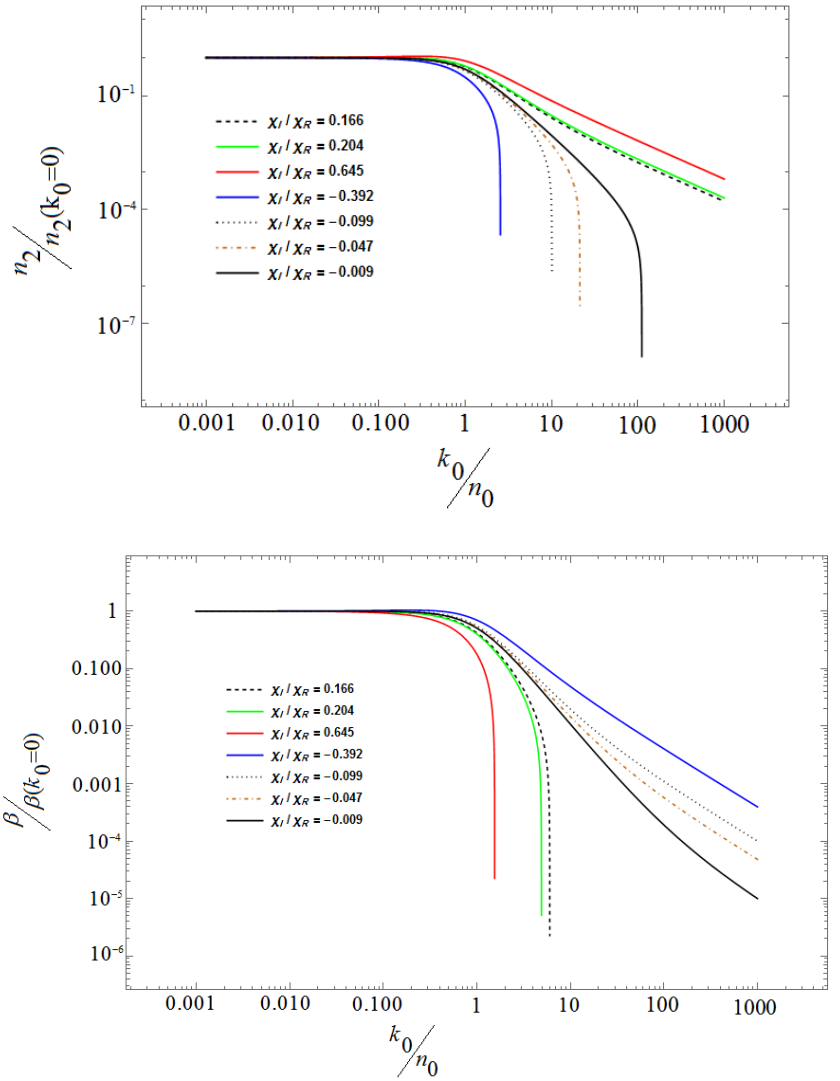

Fig. 6. Calculated $n_2/n_2(k_0 = 0)$ and $\beta/\beta_{(k0=0)}$ ratio as a function of k_0/n_0 for different indicated values of the $\chi_I^{(3)}/\chi_R^{(3)}$ ratio.

4. CONCLUSION

In this paper, we calculated the third order nonlinear susceptibilities under the effective mass approximation with intersubband transitions in the conduction band are theoretically calculated for PbS/ CdSe/ CdS spherical core-shell-shell quantum dots. Results reveal great dependence of nonlinear susceptibilities on

size of core and shell. We have also investigated analytical expressions relating the nonlinear refractive index n_2 and the nonlinear absorption coefficient β or k_2 to real and imaginary parts of the third-order nonlinear susceptibilities. It is shown in the case of the negligible absorption assumption ($k_0 = 0$), n_2 and β is greatly dependent on the k_0 / n_0 for different value of $\chi_I^{(3)} / \chi_R^{(3)}$.

REFERENCES

[1] P. Resis, S. Carayon, J. Bleuse, A. Pron, *Low polydispersity core/shell nanocrystals of CdSe/ZnSe and CdSe/ZnSe/ZnS type: preparation and optical studies*, Synthetic Metals 139, (2003) 649-652.

[2] M. Cristea, E.C. Niculescu. ,*Hydrogenic impurity states in CdSe/ZnS and ZnS/CdSe core-shell nanodots with dielectric mismatch*, Eur Phys J B 85 (2012) 191(1-13).

[3] E.C. Niculescu, M. Cristea,*Impurity states and photoionization cross section in CdSe/ZnS core–shell nanodots with dielectric confinement*, J Lumin 135 (2013) 120–127.

[4] M. Cristea, A. Radu, E.C. Niculescu, *Electric field effect on the third-order nonlinear optical susceptibility in inverted core–shell nanodots with dielectric confinement*,. J Lumin 143 (2013) 592–599.

[5] S. Gottapu and K. Muralidharan, *Room temperature synthesis of organic surfactant-free PbS and PbSe nanoparticles exhibiting NIR absorption*, New J. Chem., 40 (2016) 832-837.

[6] Z. Gui, G. Xiong, F. Gao ,*Parameter-dependent third-order nonlinear susceptibility of parabolic InGaN/GaN quantum dots*, Microelectronics Journal 38 (2007) 447–451.

[7] X. Feng, G. Xiong_, X. Zhang, H. Gao, *Third-order nonlinear optical susceptibilities associated with intersubband transitions in CdSe/ZnS core–shell quantum dots*, Physica B 383 (2006) 207–212.

[8] L. Liu, J. Li, G. Xiong, *Studies of the third-order nonlinear optical susceptibility for $In_xGa_{1-x}N$/GaN cylinder quantum dots*, Physica E 25 (2005) 466.

[9] D J. Griffiths, *Introduction to Quantum Mechanics. Boston*, Addison-Wesley; 2004.

[10] G. Guizzett, F. Filippin; E. Reguzzon, G.Samoggia, *Electrical Properties and Spectral Response of PbS_Ge Heterojunctions*, Phys. Status Solidi A 6 (1971) 605–610.

[11] R. A. Knapp, *Photoelectric Properties of Lead Sulfide in the Near and Vacuum Ultraviolet*, Phys. Rev. 132 (1963) 1891– 1897.

[12] http://www.tf.uni-kiel.de/matwis/amat/semi_en/kap_2/backbone/r2_3_1.html.

[13] M. Şahin, S. Nizamoglu, A. Emre Kavruk and H. Volkan Demir ,*Self-consistent computation of electronic and optical properties of a single exciton in a spherical quantum dot via matrix diagonalization method*, J App. Phys. 106 (2009) 43704-5.

[14] S. Khosroabadi,S. H. Keshmiri, S. Marjani ,*Design of a high efficiency CdS/CdTe solar cell withoptimized step doping, film thickness, and carrier lifetime of the absorption layer*, J. Europ. Opt. Soc. Rap. Public. 9 (2014) 14052(1-6).

[15] J.W. Haus, H.S. Zhou, I. Honma, H. Komiyama, *Quantum confinement in semiconductor heterostructure nanometer-size particles*, Phys. Rev. B 47 (1993) 1359-1365.

[16] D.J. Ben Daniel, C.B. Duke, *Space-Charge Effects on Electron Tunneling*, Phys. Rev. 152 (1968) 683-692.

[17] L.E. Brus, *A simple model for the ionization potential, electron affinity, and aqueous redox potentials of small semiconductor crystallites*, J. Chem. Phys. 79 (1983) 5566-5571.

[18] M. Kouhi, A. Vahedi, A. Akbarzadeh, Y. Hanifehpour and S. W. Joo ,*Investigation of quadratic electro-optic effects and electro-absorption process in GaN/AlGaN spherical quantum dot*, Nanoscale Research Letters 9 (2014) 131(1-6).

[19] T. Takagahara, *Excitonic optical nonlinearity and exciton dynamics in semiconductor quantum dots*, Phys. Rev. B 36 (1987) 9293.

[20] X.N. Liu and D.Z. Yao, *Parameter-dependent third-order optical nonlinearity in a CdSe/ZnS quantum dot quantum well in the vicinity of a gold nanoparticle*, Eur. Phys. J. B 78 (2010) 95–102.

[21] I. Hemdana, M. Mahdouani and R. Bourguiga, *Investigation of the third-order nonlinear optical susceptibilities associated with intersubband transitions in CdSe/ZnS/SiO_2 core/shell/shell quantum dot*, Superlattices and Microstructures 60 (2013) 336–348.

[22] R. Coso and J. Solis, *Relation between nonlinear refractive index and third order susceptibility in absorbing media*, J. Opt. Soc. Am. B. 21(3) (2004) 640-644.